Micellization Kinetics of a Novel Multi-Responsive Double Hydrophilic Diblock Copolymer Studied by Stopped-Flow pH and Temperature Jump

Yanfeng Zhang, Tao Wu, Shiyong Liu*

Double hydrophilic diblock copolymer, poly(*N*-isopropylacrylamide)-*block*-poly(2-diethylamino ethyl methacrylate) (PNIPAM-*b*-PDEA), was synthesized via reversible addition-fragmentation chain transfer (RAFT) polymerization. Containing the well-known thermo-responsive PNIPAM block and pH-responsive PDEA block, this novel diblock copolymer exhibits intriguing "schizophrenic" micellization behavior in aqueous solution, forming PDEA-core micelles at alkaline pH and room temperature, and PNIPAM-core micelles at acidic pH and elevated temperatures. The kinetics of the pH- and thermo-responsive micellization processes were studied in detail using a stopped-flow apparatus equipped with a newly developed millisecond temperature jump (mT-jump) accessory. Upon a pH jump from 4 to 12 at 25 °C, the early stages of relaxation curves monitoring the formation PDEA-core micelles can be well-fitted using a double-exponential function, leading to two characteristic relaxation time constants, τ_1 and τ_2. As τ_2 decreases with increasing polymer concentration, the slow process is thus expected to proceed via micelle fusion/fission mechanism, approaching the final equilibrium state. Upon a temperature jump from 20 to 45 °C at pH 4, the relaxation curves monitoring the formation PNIPAM-core micelles can also be well-fitted using a double-exponential function. The fast process (τ_1) is associated with the quick association of unimers into a large amount of small micelles and the formation of quasi-equilibrium micelles. τ_2 is almost independent of polymer concentration, suggesting that unimer insertion/expulsion is the main mechanism for the slow process. The protonated PDEA corona of quasi-equilibrium micelles renders the micelle fusion/fission mechanism less favorable due to electrostatic repulsion.

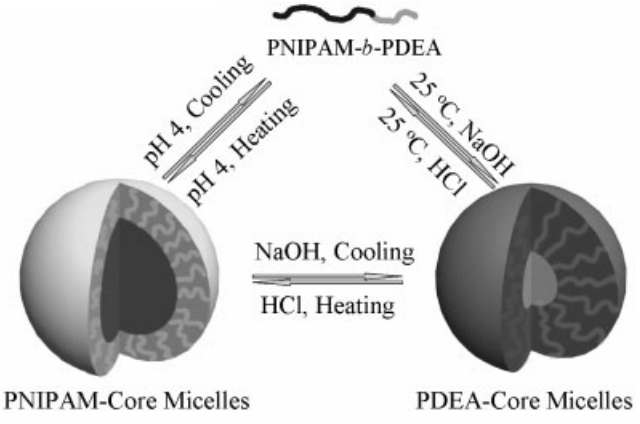

Y. Zhang, T. Wu, S. Liu
Department of Polymer Science and Engineering, Hefei National Laboratory for Physical Sciences at the Microscale, University of Science and Technology of China, Hefei, Anhui 230026, China
E-mail: sliu@ustc.edu.cn

Introduction

Double hydrophilic block copolymers (DHBCs) can self-assemble into one or more types of micellar aggregates in

Macromol. Chem. Phys. **2007**, *208*, 2492–2501

DOI: 10.1002/macp.200700293

water if solution conditions are properly adjusted.[1] Since 1998, numerous examples of novel water-soluble diblock copolymers exhibiting the so-called "schizophrenic" micellization behavior have been reported.[1–12] The micellization of "schizophrenic" block copolymers can be induced from external stimuli such as pH, ionic strength, and temperature. Among the previously studied systems, poly(*N*-isopropylacrylamide) (PNIPAM),[3,4,13] poly(propylene oxide) (PPO),[7,14] and poly(oligo(ethylene glycol) methacrylate) (PEGMA)[15] have been frequently used as the thermosensitive component; while poly[2-(diethylamino) ethyl methacrylate] (PDEA)[14,16,17] and poly(4-vinylpyridine) (P4VP)[11] are well-known as the pH-responsive block. A novel type of combination, i.e., PNIPAM-*b*-PDEA diblock copolymer, was chosen in this study, with emphasis on its "schizophrenic" micellization kinetics, studied by stopped-flow pH and temperature jump.

Most of the reports of stimuli-responsive micellization and micelle inversion of DHBCs focused on the characterization of the equilibrium micelle structures. On the other hand, theoretical and experimental studies of the dynamics of micellization are quite mature for small molecule surfactants. The Aniansson and Wall (A-W) theory has been generally accepted nowadays for the dynamics of surfactant micelles upon a small perturbation, leading to the relaxation from the initial equilibrium state to the final state via two successive processes.[18–20] An important assumption in this theory is that all changes are due to an elementary process of insertion/expulsion of individual chains ('unimers') into/out of the micelle. However, for the slower process (τ_2), i.e., micelle formation and breakup, it has been postulated that micelle fusion-fission may also be involved, especially at higher surfactant concentrations or in the presence of electrolytes.[21,22]

For block copolymers, the characteristic relaxation time for a copolymer chain to escape from the micelles has been theoretically discussed by Halperin and Alexander on the basis of scaling analysis within the context of the A-W theory.[23] Their main conclusion is that insertion/expulsion of individual chains (unimer exchange) is the only mechanism for micelle relaxation processes upon small perturbation from equilibrium state.

For large deviations from the initial state, i.e., unimer-micelle transition, Mattice et al.[24] performed computer simulations, suggesting the presence of two processes with different time scales, the volume fraction of free chains reaches its equilibrium value very quickly in the fast step, followed by a step towards the equilibrium state at a much slower rate. Dormidontova and co-workers[25] further proposed a micelle fusion/fission - unimer expulsion/entry joint mechanism for block copolymer micelle evolution, suggesting that micelle fusion/fission dominates over unimer entry/expulsion in the initial fast process; while unimer entry/expulsion mechanism dominates during the second slow process. However, Semenov et al.[26,27] recently postulated that the unimer-micelle transition can not be simply characterized by just two relaxation times, but rather by a continuous spectrum of relaxation times. They also proposed that the main route of micelle growth should involve step-by-step joining of unimers, i.e., insertion/expulsion of individual chains.

Recently, we reported the kinetics of pH-induced micellization of a stimulus-responsive ABC triblock copolymer, namely poly(glycerol monomethacrylate)-*block*-poly[2-(dimethylamino)ethyl methacrylate]-*block*-poly[2-(diethylamino)ethyl methacrylate] (PGMA-*b*-PDMA-*b*-PDEA).[28] The micellization kinetics was investigated by stopped-flow light scattering. Upon jumping from pH 4 to 12, the early stages of micellization occurred via two successive processes. The first fast process (τ_1) is associated with the formation of quasi-equilibrium micelles and the second slow process (τ_2) is associated with micelle formation and break-up, approaching the final equilibrium state. τ_2 is almost independent of polymer concentration, indicating that the slow process proceeds mainly via the unimer insertion/expulsion mechanism. We also studied the micellar formation and inversion kinetics of a schizophrenic diblock copolymer of poly(4-vinylbenzoic acid)-*block*-poly[*N*-(morpholino)ethyl methacrylate] (VBA-*b*-MEMA), induced by a combination of pH and ionic strengths.[29]

Concerning the thermoresponsive micellization, Honda et al.[30,31] studied the kinetics of micellization after quenching from unimer to micelle region for poly(α-methylstyrene)-*block*-poly(vinylphenethyl alcohol) (PMS-*b*-PVPh) in benzyl alcohol. Micellar self-assembly in this case was very slow, which enabled the process to be monitored by static and dynamic laser light scattering (LLS). The limitation of the LLS technique is that it needs a relatively long thermal equilibration period, so the kinetics of the early stages was missing.

The kinetics of thermoresponsive micellization of DHBCs has never been reported, probably due to the lack of suitable techniques to monitor the fast formation of micelles. Previous temperature jump studies of surfactant micellization dynamics involves laser flash or electric discharge,[32] limited by the fact that only small temperature jump can be realized and the shifted temperature can not be maintained for a relatively long time, i.e., the system naturally cools down after 10–100 ms, which is surely not enough for monitoring the relaxation kinetics of polymeric micelles. Coupling conventional stopped-flow apparatus with temperature-jump accessory would be advantageous for monitoring the thermoresponsive micellization kinetics of DHBCs, as the time window can cover from the dead time of stopped-flow (2–3 ms) to extremely long time period.

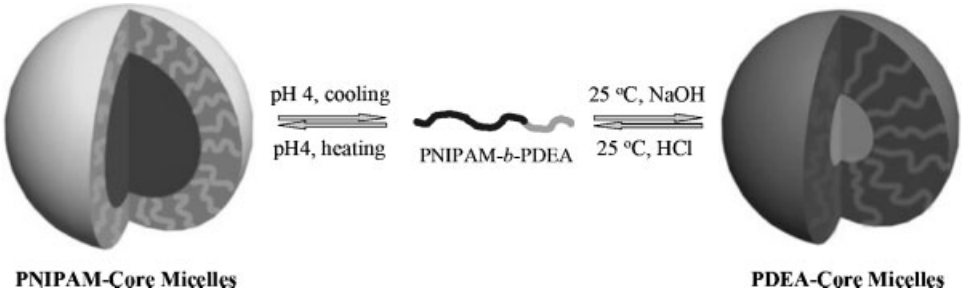

Scheme 1. Schematic illustration of the thermo- and pH-responsive micellization of PNIPAM$_{232}$-*b*-PDEA$_{106}$.

Herein, we synthesized a novel thermo- and pH-responsive diblock copolymer, PNIPAM-*b*-PDEA, via reversible addition-fragmentation chain transfer (RAFT) polymerization.[33,34] This diblock copolymer exhibits intriguing "schizophrenic" micellization behavior in aqueous solution upon dually playing with external pH and temperature. At room temperature, the copolymer chains molecularly dissolve at pH $<$ 6.5 and form PDEA-core micelles at pH $>$ 7.5. Above the lower critical solution temperature (LCST) of the PNIPAM block, copolymer chains self-assemble into structurally inverted PNIPAM-core micelles at pH $<$ 6.5 (Scheme 1). ^{1}H NMR and LLS were employed to characterize the equilibrium micelle structures. Moreover, the pH- and thermo-responsive micellization kinetics was studied in detail using a stopped-flow apparatus equipped with a newly developed millisecond temperature jump (mT-jump) accessory.

Experimental Part

Materials

N-Isopropylacrylamide (NIPAM) (97%, Tokyo Kasei Kagyo Co.) was purified by recrystallization from a mixture of benzene and hexane (1/3, v/v). 2-(Diethylamino)ethyl methacrylate (DEA) was obtained from Aldrich. It was passed through basic alumina columns, then vacuum-distilled from CaH_2, and stored at $-20\,^{\circ}C$ prior to use. 2-Cyanoprop-2-yl dithiobenzoate (CPDB) was synthesized according to literature method.[35] 2,2′-Azoisobutyronitrile (AIBN) was recrystallized from ethanol. Petroleum ether, hexane, and tetrahydrofuran (THF) were dried by refluxing over sodium and distilled prior to use.

RAFT Polymerization of NIPAM

The RAFT polymerization of NIPAM was conducted in a sealed ampoule. In a typical run, NIPAM (5.08 g, 45 mmol), CPDB (33.2 mg, 0.15 mmol), and AIBN (4.9 mg, 0.03 mmol) were charged into the glass ampoule containing THF at the molar ratio of 1 500:5:1. The mixture was degassed through three freeze-thaw cycles. The ampoule was then sealed under vacuum, and kept in an oil bath at 80 °C to conduct the polymerization. After 24 h, the ampoule was quenched into liquid nitrogen to stop the polymerization. The ampoule was broken, and THF was added to dilute the mixture before it was precipitated into excess diethyl ether. This precipitation procedure was repeated three times. The resulting slightly pink powder was dried overnight under vacuum at room temperature, and the yield was ≈80%. The molecular weight and molecular weight distribution of PNIPAM homopolymer were determined by SEC: $\overline{M}_n = 32\,500$, $\overline{M}_w/\overline{M}_n = 1.06$. The actual degree of polymerization (DP) of the PNIPAM homopolymer was determined to be 232 by ^{1}H NMR.

Synthesis of PNIPAM-*b*-PDEA

The RAFT polymerization of DEA using PNIPAM macroRAFT agent was conducted in a sealed ampoule. In a typical run, PNIPAM (1.03 g, 0.04 mmol), DEA (1.33 g, 7.2 mmol), and AIBN (0.8 mg, 0.005 mmol) were charged into the glass ampoule containing THF at the molar ratio of 8:1 440:1. The mixture was degassed through three freeze-thaw cycles. The ampoule was then sealed under vacuum, and kept in an oil bath at 80 °C to conduct the polymerization. After 20 h, the ampoule was quenched into liquid nitrogen to stop the polymerization. The ampoule was broken, and THF was added to dilute the mixture. After evaporating all the solvent, residual DEA monomer was removed by dialysis (MW cutoff, 14 000 Da) against slight acidic water (pH 5). After drying in a vacuum oven overnight, slightly pink and viscous solids were obtained with a yield of 68%. The molecular weight and molecular weight distribution of PNIPAM- *b*-PDEA diblock copolymer were determined by SEC: $\overline{M}_n = 42\,800$, $\overline{M}_w/\overline{M}_n = 1.14$. The DP of the PDEA was determined to be 106 by ^{1}H NMR. The obtained diblock copolymer was denoted PNIPAM$_{232}$-*b*-PDEA$_{106}$.

Characterization

Nuclear Magnetic Resonance (NMR) Spectroscopy

All ^{1}H NMR spectra were recorded using a Bruker 300 MHz spectrometer. PNIPAM-*b*-PDEA copolymer was analyzed in D_2O. DCl and NaOD were used for adjusting pH.

Size Exclusion Chromatography

Molecular weight distributions were determined by SEC using a series of three linear Styragel columns HT2, HT3, HT5 and a column temperature of 60 °C. Waters 1515 pump and Waters 2414 differential refractive index detector (set at 30 °C) was used. The eluent was DMF at a flow rate of 1.0 ml · min^{-1}. A series of low polydispersity polystyrene standards were employed for the SEC calibration. $\overline{M}_n$ and $\overline{M}_w$ were determined using universal calibration.

Macromol. Chem. Phys. **2007**, *208*, 2492–2501

Macromolecular Journals

DOI: 10.1002/macp.200700293

Laser Light Scattering (LLS)

A commercial spectrometer (ALV/DLS/SLS-5022F) equipped with a multi-tau digital time correlator (ALV5000) and a cylindrical 22 mW UNIPHASE He-Ne laser ($\lambda_0 = 632$ nm) as the light source was employed for dynamic and static LLS measurements. In static LLS, we can obtain the weight-average molar mass ($\overline{M}_w$) and the *z*-average root- mean square radius of gyration ($\langle R_g^2 \rangle^{1/2}$ or written as $\langle R_g \rangle$) of polymer chains or aggregates in a dilute solution from the angular dependence of the excess absolute scattering intensity, known as Rayleigh ratio $R_{vv}(q)$. The specific refractive index increments, d*n*/d*C* values, were determined to be 0.125 $mL \cdot g^{-1}$ (pH 4, 45 °C) and 0.170 $mL \cdot g^{-1}$ (pH 10, 25 °C) for $PNIPAM_{232}$-*b*-$PDEA_{106}$ in aqueous solution by a precise differential refractometer at a wavelength of 632 nm.[36] The molar mass of block copolymer micelles was measured from only one concentration (2×10^{-4} $g \cdot mL^{-1}$), and the extrapolation to zero concentration was not conducted. Thus, the obtained $\overline{M}_w$ should only be considered as apparent values, denoted as $\overline{M}_{w,app}$.

Stopped-Flow pH and Temperature Jump with Light Scattering Detection

Stopped-flow studies were carried out using a Bio-Logic SFM300/S stopped-flow instrument. The SFM-3/S is a three-syringe (10 mL) instrument in which all step-motor-driven syringes (S1, S2, S3) can be operated independently to carry out single- or double-mixing. The SFM-300/S stopped-flow device is attached to the MOS-250 spectrometer; kinetic data were fitted using the program Biokine (Bio-Logic). For the light scattering detection at a scattering angle of 90°, both the excitation and emission wavelengths were adjusted to 335 nm with 10 nm slits. Using FC-15 flow cells the typical dead time is 2.6 ms.

The millisecond temperature jump (mT-jump) accessory is equipped with a standard Bio-Logic stopped-flow observation cell, three thermoelectric Peltier elements are used to control the initial temperatures of the two solutions and that of the observation cell after mixing. The temperature of the mixed solution was calibrated to be the same as the observation cell (Peltier controlled) with the aid of a thermosensitive fluorescent dye, *N*-acetyl-L-tryptophanamide (NATA). The precision of the temperature jump is within ±0.1 °C, and the temperature stability in the observation cell after temperature jump was <1% in 30 s.

Results and Discussion

Synthesis of PNIPAM-*b*-PDEA

The target block copolymer was synthesized by successive RAFT polymerization of NIPAM and DEA. First, NIPAM was polymerized at 80 °C using 2-cyanoprop-2-yl dithiobenzoate (CPDB) as the RAFT agent. ^{1}H NMR spectrum of PNIPAM in $CDCl_3$ reveals the presence of signals characteristic of PNIPAM at $\delta = 5.8$–7.0 (–CON*H*–), 4.0 (–CONHC*H*–), and 1.2 ppm (–CH_3). Signals at $\delta = 7.9$, 7.6, and 7.4 ppm are ascribed to protons of dithiobenzoyl group located at the PNIPAM chain end. SEC analysis in DMF revealed a

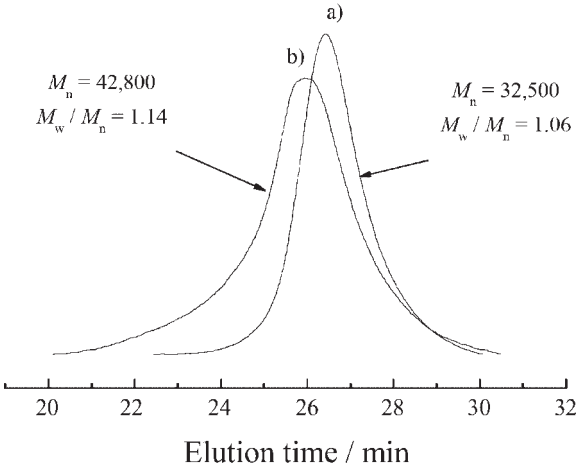

Figure 1. SEC traces of (a) PNIPAM macroRAFT agent and (b) $PNIPAM_{232}$-*b*-$PDEA_{106}$ diblock copolymer.

mono-modal peak with $\overline{M}_n \approx 32\,500$, and a polydispersity, $\overline{M}_w/\overline{M}_n$, of 1.06 (Figure 1). The actual degree of polymerization, DP, of PNIPAM was determined to be 232 by ^{1}H NMR.

The obtained PNIPAM was employed as macroRAFT agent for the polymerization of DEA monomer, leading to the formation of PNIPAM-*b*-PDEA diblock copolymer. ^{1}H NMR spectrum of the final product in D_2O at pH = 4.0 (Figure 2a) reveals the presence of characteristic signals of both blocks. Most importantly, SEC trace in Figure 1 clearly show that the elution peak of PNIPAM-*b*-PDEA shifts to higher molecular weight compared to that of PNIPAM precursor, indicating the successful preparation of the diblock copolymer. The elution peak of the diblock copolymer is relatively symmetric, revealing an $\overline{M}_w/\overline{M}_n$ of 1.14.

"Schizophrenic" Micellization of PNIPAM-*b*-PDEA

PDEA homopolymer is a weak polybase and its conjugated acid has a pK_a of ≈7.3. It is water-insoluble at neutral or alkaline pH. Below pH 6, it is soluble as a weak cationic polyelectrolyte due to protonation of the tertiary amine groups. PNIPAM homopolymer dissolves in cold and dilute aqueous solution but becomes insoluble at ≈32 °C due to the lower critical solution temperature (LCST) phase behavior. Thus, it was quite expected that $PNIPAM_{232}$-*b*-$PDEA_{106}$ will exhibit thermoresponsive and pH-responsive "schizophrenic" micellization behavior in aqueous solution.[7]

Figure 2 shows the ^{1}H NMR spectra recorded for $PNIPAM_{232}$-*b*-$PDEA_{106}$ in D_2O at different pH and temperatures. Both blocks are fully solvated at pH 4 and 25 °C, and all the signals characteristic of PNIPAM and PDEA blocks are visible. Upon adjusting the solution pH to 9,

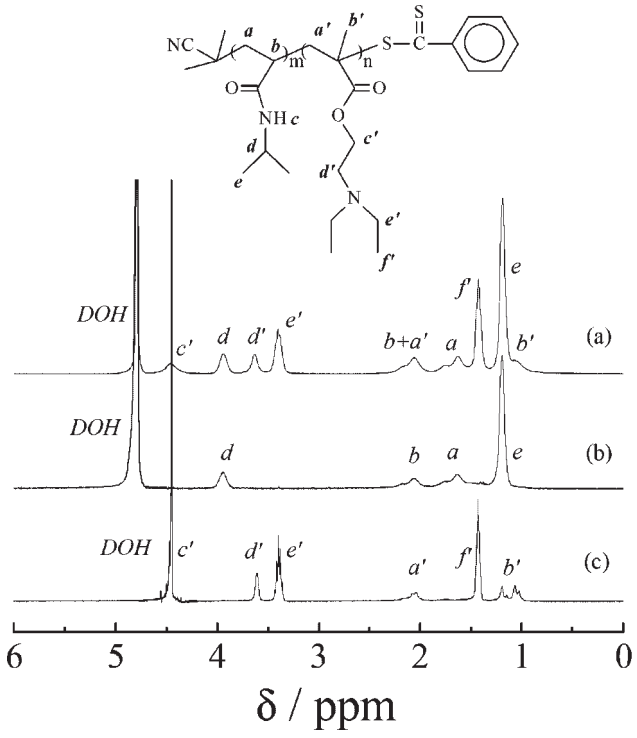

Figure 2. ^{1}H NMR spectra of the PNIPAM$_{232}$-*b*-PDEA$_{106}$ diblock copolymer in D_2O: (a) at pH 4, 25 °C; (b) at pH 9, 25 °C; (c) at pH 4, 45 °C.

signals at 3.3–3.7 and 1.1 ppm, which are characteristic of PDEA, completely disappeared (Figure 2b), while the signal characteristic of PNIPAM ($\delta = 4.0$ ppm) is still visible. This indicates the formation of PDEA-core micelles with the corona consisting of the PNIPAM block. On the other hand, increasing the temperature to 45 °C at pH 4 leads to the disappearance of the characteristic PNIPAM signals at $\delta = 4.0$ and 1.5 ppm (Figure 2c), suggesting the formation of PNIPAM-core micelles. This conclusion was further corroborated by the fact that signals characteristic of PDEA at $\delta = 3.3$–3.7 and 1.1 ppm are clearly evident (Figure 2c). A schematic illustration of the "schizophrenic" micellization behavior of PNIPAM$_{232}$-*b*-PDEA$_{106}$ was shown in Scheme 1.

Figure 3a shows the pH-dependence of dynamic LLS results for PNIPAM$_{232}$-*b*-PDEA$_{106}$ at a concentration of 0.2 g·L^{-1}. Below pH 6–7, the diblock copolymer molecularly dissolve, with an intensity-average hydrodynamic diameter, $\langle R_h \rangle$, of ≈10 nm and very low scattering intensity. Upon addition of NaOH, micellization occurred above pH 7, as indicated by the bluish tinge that is characteristic of micellar solutions. On the basis of chemical intuition and previous ^{1}H NMR results, these micelles are expected to have a core-corona structure, with the DEA block occupying the micelle core and PNIPAM block forming the corona (Scheme 1). Above pH 8, the micelle size remains almost constant, and the $\langle R_h \rangle$ is ≈67 nm. The micellar solution remains colloidally stable over 3 months at temperatures below 30 °C. Above this critical temperature, further aggregation between micelles aggregation takes place due to the thermal phase transition of the PNIPAM corona. Moreover, the PDEA-core micelles are quite monodisperse, with polydispersities (μ_2/Γ^2) typically less than 0.10 (Figure 3a). Static LLS studies of the PDEA-core micelles at pH 10 revealed an apparent radius of gyration, $\langle R_g \rangle$, of 62 nm and an apparent weight-average molar mass, $\overline{M}_{w,app}$, of 8.7×10^7 g·mol^{-1}. The aggregation number per micelle, N_{agg}, was thus calculated to be ≈1 660. The chain density (ρ) of micelles was ≈0.115 g·cm^{-3}.

Figure 3b shows the temperature dependence of dynamic LLS results for the PNIPAM$_{232}$-*b*-PDEA$_{106}$ diblock copolymer at pH 4 and a polymer concentration of 0.2 g·L^{-1}. The block copolymer molecularly dissolves in water below 36 °C. Above that, micellization starts to take place, accompanied with a dramatic increase of $\langle R_h \rangle$. Dynamic LLS only revealed one population corresponding to micelles above 42 °C, the micelle size remains almost constant, with $\langle R_h \rangle$ of ≈75 nm. The micelles should possess a core-corona structure, with the core consisting of

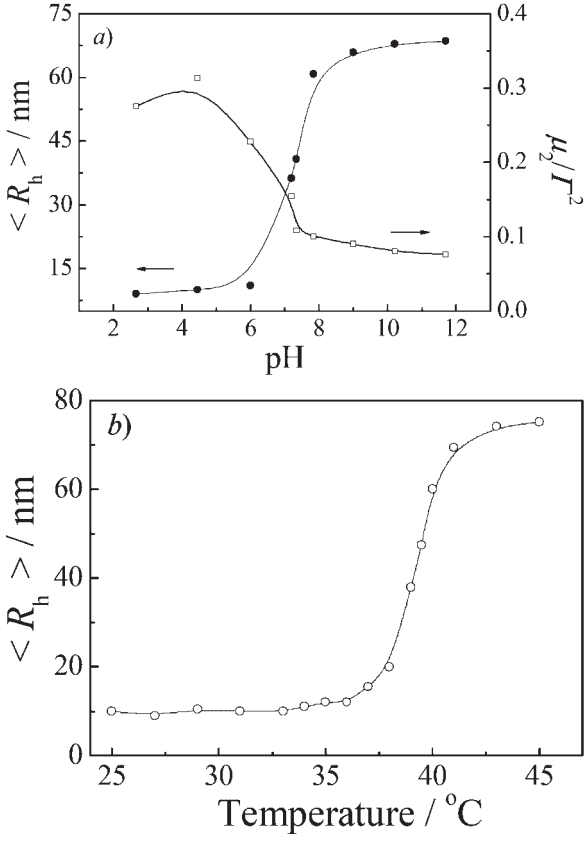

Figure 3. a) Variation of intensity-average hydrodynamic radius, $\langle R_h \rangle$, and μ_2/Γ^2 with solution pH for PNIPAM$_{232}$-*b*-PDEA$_{106}$ at 25 °C. b) Variation of intensity-average hydrodynamic radius, $\langle R_h \rangle$, with temperature for PNIPAM$_{232}$-*b*-PDEA$_{106}$ at pH 4. The polymer concentration was 0.2 g·L^{-1}.

Macromol. Chem. Phys. **2007**, *208*, 2492–2501

Macromolecular Journals

DOI: 10.1002/macp.200700293

PNIPAM and the shell of PDEA (Scheme 1). At 45 °C, static LLS revealed an average radius of gyration, $\langle R_g \rangle$, of 73 nm and an $\overline{M}_{w,app}$ of 7.4×10^7 g · mol^{-1}. The N_{agg} of PNIPAM-core micelles was calculated to be 1 410, and the average chain density of micelles was 0.070 g · cm^{-3}. For PNIPAM-core micelles (pH 4), the coronas consist of PEEA chains in their fully protonated state. Thus, the lower micelle density of PNIPAM-core micelles compared to that of PDEA-core micelles might be due to the charge repulsion between neighboring PDEA chains, preventing the dense packing of PNIPAM blocks within the micelle cores.

Kinetics of pH- and Thermo-Responsive Micellization

The kinetics of the "schizophrenic" micellization of PNIPAM$_{232}$-*b*-PDEA$_{106}$ diblock copolymer was further studied employing a stopped-flow apparatus equipped with a newly developed millisecond temperature jump (mT-Jump) accessory. Thus, both pH and temperature jumps can be conveniently realized, with a typical dead time of 2–3 ms. Moreover, the measurements can be extended up to a few hours. The combination of stopped-flow and temperature-jump was thus superior to temperature-jumps induced by laser flash or electric discharge.[32] In the latter, the temperature shift can be only maintained up to 10–100 ms, which is surely not enough for monitoring the growth kinetics of polymeric aggregates.

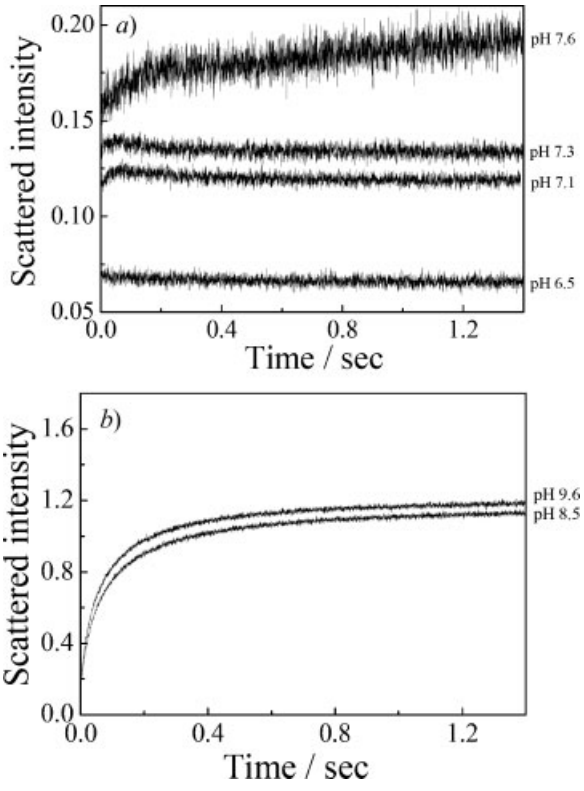

Figure 4. Time dependence of the scattered light intensities of aqueous solution of PNIPAM$_{232}$-*b*-PDEA$_{106}$ diblock copolymer caused by a pH jump from 4 to different final pH. The final copolymer concentration was fixed at 0.2 g · L^{-1}.

Kinetics of pH-Induced Formation and Breakup of PDEA-Core Micelles

Figure 4 shows the time dependence of scattering light intensities after a jump from pH 4 to different final pH. If the final pH was below 6.5, the relaxation curve remains a straight line. Diblock copolymer chains exist as unimers; thus, we do not observe any relaxation processes. Upon a pH jump from 4 to 7.1–7.3, the light scattering intensities increase initially and gradually approach the equilibrium value (Figure 4a). This was in agreement with our previous studies of the micellization kinetics of PGMA-*b*-PDMA-*b*-PDEA triblock copolymer.[28]

Above pH 8.5, only relaxation processes with quite large positive amplitudes was observed (Figure 4b). The scattering intensity shows an initially fast increase, and then the increase gradually slow down. Preliminary experiments at extended time period after stopped-flow mixing revealed that the scattering intensity still shows a weak increase even after 20 min, indicating that the final equilibrium state has not reached yet within the experimental duration.

It is known that for some systems, such as PMS-*b*-PVPh, it takes several days to relax into the equilibrium state.[30,31] Semenov et al.[26,27] proposed theoretically that the unimer-micelle transition can not be characterized by just two relaxation times, but rather by a continuous spectrum of relaxation times, owing to increasing energy barrier with growing micelle aggregation numbers. Most importantly, the growing micelles therefore may never reach the near-equilibrium size, and their growth may be arrested at an intermediate stage. For kinetic studies in the current case, we only focused on the early stages of the micelle formation process, during which the most dramatic changes occurs. At later stages of unimer-micelle transition, we believe that the relaxation into the final equilibrium state will follow equilibrium exchange kinetics, the study of which has been relatively mature.[37–39] Lund et al.[40,41] recently revealed that the equilibrium exchange kinetics follows logarithmic law by time-resolved small angle neutron scattering (SANS). The only concern in their experimental design is that the kinetic information during the first 1–2 min was missing.

At early stages of micellization, the time dependence of the scattering light intensity, I_t, can be converted to a normalized function, namely, $(I_\infty - I_t)/I_\infty$ versus t, where I_∞ is the value of I_t at long time.[42] Empirically, it was found that such a function could be well fitted by a double

exponential function:

$$(I_\infty - I_t)/I_\infty = c_1 e^{-t/\tau_1} + c_2 e^{-t/\tau_2} \quad (1)$$

where c_1 and c_2 are the normalized amplitudes ($c_2 = 1 - c_1$), τ_1 and τ_2 are the characteristic relaxation time of two processes, $\tau_1 < \tau_2$. The mean micelle formation constant, τ_f, can be calculated as

$$\tau_f = c_1\tau_1 + c_2\tau_2 \quad (2)$$

Both τ_1 and τ_2 have positive amplitudes. Upon a jump from pH 4 to ≈12 at a copolymer concentration of 0.2 $g \cdot L^{-1}$, τ_1 and τ_2 are 33 ms and 176 ms, respectively. The calculated τ_f based on Equation (2) is 95 ms.

The fast process (τ_1) with positive amplitude is associated with the quick association of unimers into a large amount of small micelles and their further growth into quasi-equilibrium micelles. The aggregation number per micelles abruptly increases during this process, leading to fast changes of scattering intensities. At the end of the first process, the unimer concentration comes close to the critical micellization concentration (cmc). According to Dormidontova et al.,[25] micelle fusion/fission mechanism may be involved in the growth from small micelles into quasi-equilibrium micelles.

The slow process (τ_2) should be ascribed to relaxation of the number of micelles involving micelle formation/breakup, approaching the final equilibrium state. At extended time period beyond the experimental duration, we can not exclude the possibility that more relaxation processes exist due to increasing energy barriers.[26,27]

We further studied the copolymer concentration dependence of τ_1 and τ_2 upon pH jump from 4 to 12 (Figure 5). If the final polymer concentration was below 0.05 $g \cdot L^{-1}$, we do not observe any relaxation process, and the dynamic curve remains a straight line. For polymer concentrations >0.1 $g \cdot L^{-1}$, relaxation processes with positive amplitudes were typically observed. All the dynamic curves in Figure 5 can be well-fitted with a double exponential function. τ_1, τ_2, and the calculated τ_f based on Equation (2) were shown in Figure 6. τ_1 and τ_2 was in the range 20–40 and 140–200 ms, respectively. Both of them decrease with increasing polymer concentration.

The slow process (τ_2) is associated with micelle formation/breakup, leading to micelles with larger aggregations numbers and lower number density of micelles. Here, τ_2 decreases with increasing copolymer concentration, which suggests that the micelle formation/breakup process proceeds via the fusion/fission mechanism. Previously, we studied the pH-induced micellization kinetics of $PGMA_{45}$-*b*-$PDMA_{34}$-*b*-$PDEA_{52}$, and τ_2 is almost independent of polymer concentration, indicating that the slow process proceeds mainly through the insertion/expulsion of individual chains.[28] The different mechanism in the slow process should be ascribed to different chain lengths of the insoluble PDEA block. Chain entanglement in the PDEA core of $PNIPAM_{232}$-*b*- $PDEA_{106}$ micelles may lead to larger energy barriers for the unimer insertion/expulsion mechanism.[25]

We have also studied the micelle dissociation kinetics upon a pH jump from 10 to various final pH (Figure 7). The final diblock copolymer concentration was fixed at 0.4 $g \cdot L^{-1}$. At final pH ≥ 9, the relaxation curve remains a straight line, indicating the absence of any relaxation processes. At the final pH ≈ 8–8.5, the scattering intensities

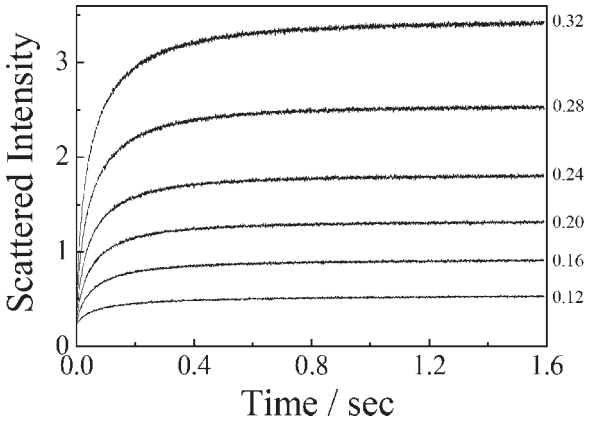

Figure 5. Time dependence of the scattered light intensities of aqueous solution of $PNIPAM_{232}$-*b*-$PDEA_{106}$ diblock copolymer caused a pH jump from 4 to 12 at different final polymer concentrations ($g \cdot L^{-1}$).

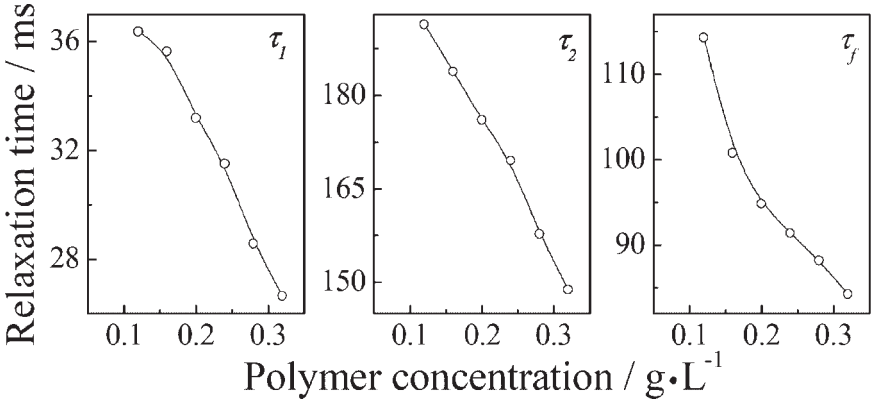

Figure 6. Double exponential fits obtained from the micelle formation processes at different diblock copolymer concentrations. The experimental conditions are the same as those described in Figure 5.

DOI: 10.1002/macp.200700293

gradually decrease with the lapse of time. Further lowering the final pH (≈6.9–7.8) led to more dramatic decrease of scattering intensities. In all the above cases, the lowering of solution pH led to micelles with lower aggregation numbers due to the gradual protonation of the PDEA core. At the final pH < 6, we can clearly see that all the micelles dissociate into unimers within ≈40 ms. The lower the final solution pH, the faster the dissociation, and the larger the loss of amplitude within the stopped-flow dead time (≈2–3 ms).

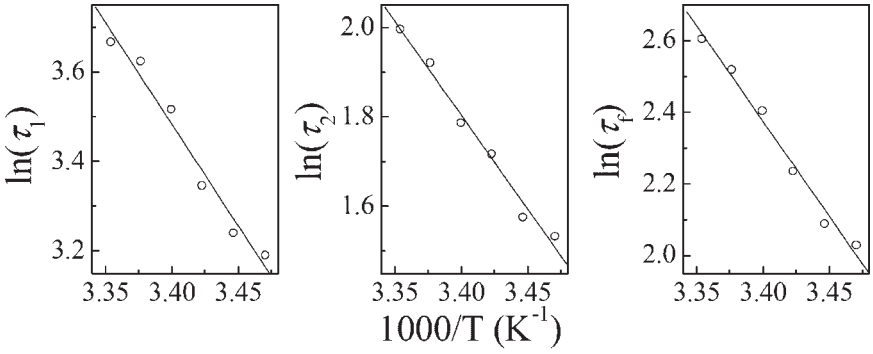

Figure 8. Arrhenius plots of τ_1, τ_2, and τ_f of the pH-induced micellization processes of $PNIPAM_{232}$-*b*-$PDEA_{106}$ upon a pH jump from 4 to 12. The final copolymer concentration was fixed at 0.2 g · L^{-1}.

Figure 8 shows the temperature dependence of τ_1, τ_2, and τ_f in the micelle formation process upon the pH-jump from 4 to 12 at a fixed polymer concentration of 0.2 g · L^{-1}. It is quite expected that τ_1, τ_2, and τ_f decrease with increasing temperature, indicating that energy barriers are encountered during the micellization process. Arrhenius plots in Figure 8 yielded activation energies of 37.8 kJ · mol^{-1}, 34.9 kJ · mol^{-1}, and 44.3 kJ · mol^{-1} for relaxation processes associated with τ_1, τ_2, and τ_f, respectively. Processes associated with τ_1 and τ_2 have similar activation energies, imply that the micelle fusion/fission mechanism was involved in both cases.

Kinetics of Thermo-Induced Formation of PNIPAM-Core Micelles

Figure 9 shows the time dependence of scattering intensities upon jumping from 20 °C to different final temperatures. The copolymer concentration after mixing was fixed at 0.1 g · L^{-1}. If the final temperature was <34 °C, the relaxation curve remains a straight line. Diblock copolymer chains exist as unimers, and we do not observe any relaxation processes. Upon temperature jump from 20 to 35 °C, the scattering intensities gradually increase and stabilize out after ≈80–100 s. When the final temperature was in the range of 37.5–40 °C, the scattering intensities show an abrupt increase within the first 5 s and then slightly decrease. If the final temperature was in the range 42.5–45 °C, only relaxation processes with quite large positive amplitudes were observed. The scattering intensities continuously increase, although the increase was getting slower and slower with time.

It should be noted that at a final temperature >40 °C, the equilibrium scattered light intensity within the time window of stopped-flow T-jump measurements actually decreases with increasing final temperatures (Figure 9). This is in contradiction with the temperature-dependent LLS results (Figure 3b), in which the scattered light intensity at 45 °C is ≈10% higher than that at 40 °C. We tentatively ascribe this apparent discrepancy to the

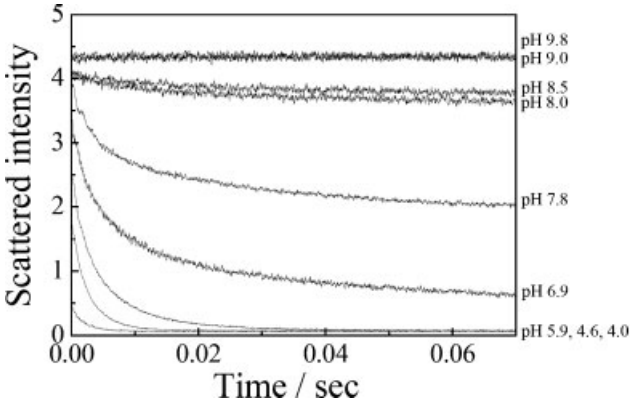

Figure 7. Time dependence of the scattered light intensities of aqueous solution of $PNIPAM_{232}$-*b*-$PDEA_{106}$ diblock copolymer caused by a pH jump from 10 to different final pH. The final copolymer concentration was fixed at 0.4 g · L^{-1}.

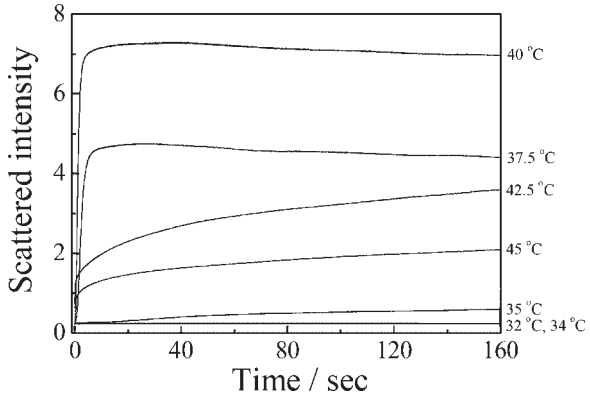

Figure 9. Time dependence of the scattered light intensities of aqueous solutions of $PNIPAM_{232}$-*b*-$PDEA_{106}$ diblock copolymer at pH 4 upon a temperature jump from 20 °C to different final temperatures. The final copolymer concentration was fixed at 0.1 g · L^{-1}.

different heating rates between LLS and stopped-flow T-jump techniques. In LLS measurements, each data point upon a temperature increase is obtained after the measured $\langle R_h \rangle$ value gets stable (Figure 3), which typically takes ≈30 min. Thus, LLS results reflect a slow evolution of micelle size and N_{agg} with increasing temperatures. In stopped-flow T-jump experiments, the temperature increase from 20 to 45 °C occurs within a few milliseconds. This might lead to effective competition between intrachain collapse and interchain aggregation of PNIPAM blocks during thermo-induced micellization.[43] In stopped-flow T-jump, the higher the final temperatures, the larger the hydrophobicity of PNIPAM block, the more prominent of intrachain collapse over that of interchain aggregation, and consequently the formation of PNIPAM-core micelles with smaller N_{agg}.The dynamic curves upon temperature jump from 20 to 45 °C at different final copolymer concentration were shown in Figure 10. All the dynamic curves in Figure 10 can be well-fitted with a double exponential function. τ_1, τ_2, and the calculated τ_f based on Equation (2) were shown in Figure 11. τ_1 was in the range of 1–3 s, and it decreased with increasing polymer concentration.τ_2 was in the range of 20–25 s, and it was almost independent of copolymer concentrations.

The fast process (τ_1) can be similarly ascribed to the quick association of unimers into large amounts of small micelles and the formation of quasi-equilibrium micelles.

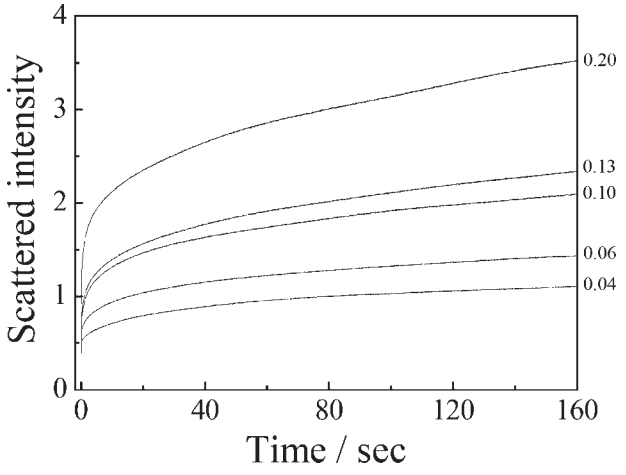

Figure 10. Time dependence of the scattering light intensities of aqueous solutions of $PNIPAM_{232}$-*b*-$PDEA_{106}$ diblock copolymer at different final polymer concentrations ($g \cdot L^{-1}$) and pH 4 caused by a temperature jump from 20 to 45 °C.

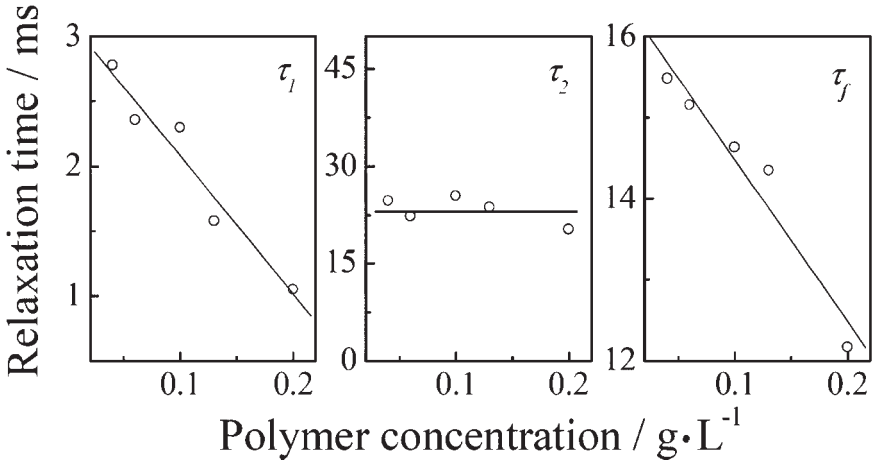

Figure 11. Double exponential fits obtained from the micelle formation processes at different $PNIPAM_{232}$-*b*-$PDEA_{106}$ diblock copolymer concentrations. The experimental conditions are the same as those described in Figure 10.

The slow process (τ_2) is associated with micelle formation/breakup, leading to micelles with larger aggregations numbers and lower number density of micelles. τ_2 was independent of copolymer concentrations, suggesting that the unimer insertion/expulsion is the dominating mechanism for the micelle growth. At pH 4, the PDEA corona of PNIPAM-core quasi-equilibrium micelles are fully protonated, the electrostatic repulsion of charged micelles must lead to large activation energy barrier for micelle fusion; thus, the unimer insersion/expulsion mechanism in the slow process was highly favored.

Conclusion

Containing the well-known thermo- and pH-responsive blocks, poly(*N*-isopropylacrylamide)-*block*-poly(2-diethylamino ethyl methacrylate) (PNIPAM-*b*-PDEA) exhibits intriguing "schizophrenic" micellization behavior in aqueous solution upon dually playing with external pH and temperature. At room temperature, the copolymer chains molecularly dissolve at pH < 6.5 and form PDEA-core micelles at pH > 7.5. Above the lower critical solution temperature (LCST) of the PNIPAM block, copolymer chains self-assemble into structurally inverted PNIPAM-core micelles at pH < 6.5.

The kinetics of the pH- and thermo-responsive micellization processes were studied in detail using the stopped-flow apparatus equipped with a newly developed millisecond temperature jump (mT-jump) accessory. Upon a pH jump from 4 to 12 at 25 °C, the relaxation curves monitoring the formation PDEA-core micelles can be well-fitted using a double-exponential function, leading to two characteristic relaxation time constants, τ_1 and τ_2, which can be ascribed to the formation of quasi-equilibrium micelles and the

Macromol. Chem. Phys. **2007**, *208*, 2492–2501

Macromolecular Journals
DOI: 10.1002/macp.200700293

micelle formation/breakup, respectively. As τ_2 decrease with increasing polymer concentration, we propose that the slow process proceeds via micelle fusion/fission mechanism. Chain entanglement in the PDEA core of block copolymer micelles may lead to larger energy barriers for the unimer insertion/expulsion mechanism.

Upon a temperature jump from 20 to 45 °C at pH 4, the relaxation curves monitoring the formation PNIPAM-core micelles can also be well-fitted using a double-exponential function. The fast process (τ_1) is associated with the quick association of unimers into a large amount of small micelles and the formation of quasi-equilibrium micelles. τ_2 is almost independent of the polymer concentration, suggesting that unimer insertion/expulsion is the main mechanism for the slow process. The protonated PDEA corona of quasi-equilibrium micelles renders the micelle fusion/fission mechanism less favorable due to electrostatic repulsion.

Acknowledgements: This work was financially supported by an Outstanding Youth Fund (50425310) and research grants (20534020, 20674079) from the *National Natural Scientific Foundation of China* (NNSFC), and the "Bai Ren" Project of the *Chinese Academy of Sciences*.

Received: May 25, 2007; Revised: August 2, 2007; Accepted: August 3, 2007; DOI: 10.1002/macp.200700293

Keywords: double hydrophilic block copolymer; kinetics (polym.); micellization; self-assembly; stopped-flow; temperature-jump

[1] H. Colfen, *Macromol. Rapid Commun.* **2001**, *22*, 219.
[2] J. Rodriguez-Hernandez, S. Lecommandoux, *J. Am. Chem. Soc.* **2005**, *127*, 2026.
[3] M. Arotcarena, B. Heise, S. Ishaya, A. Laschewsky, *J. Am. Chem. Soc.* **2002**, *124*, 3787.
[4] J. Virtanen, M. Arotcarena, B. Heise, S. Ishaya, A. Laschewsky, H. Tenhu, *Langmuir* **2002**, *18*, 5360.
[5] X. Andre, M. F. Zhang, A. H. E. Muller, *Macromol. Rapid Commun.* **2005**, *26*, 558.
[6] C. D. H. Alarcon, S. Pennadam, C. Alexander, *Chem. Soc. Rev.* **2005**, *34*, 276.
[7] V. Butun, S. Liu, J. V. M. Weaver, X. Bories-Azeau, Y. Cai, S. P. Armes, *React. Funct. Polym.* **2006**, *66*, 157.
[8] Q. Bo, Y. Zhao, *J. Polym. Sci., Part A: Polym. Chem.* **2006**, *44*, 1734.
[9] G. Mountrichas, S. Pispas, *Macromolecules* **2006**, *39*, 4767.
[10] S. Pispas, *J. Polym. Sci., Part A: Polym. Chem.* **2006**, *44*, 606.
[11] W. Q. Zhang, L. Q. Shi, R. J. Ma, Y. L. An, Y. L. Xu, K. Wu, *Macromolecules* **2005**, *38*, 8850.
[12] S. Minko, "*Responsive Polymer Materials: Design and Applications*", Blackwell Publishing, Ames 2006.
[13] C. M. Schilli, M. F. Zhang, E. Rizzardo, S. H. Thang, Y. K. Chong, K. Edwards, G. Karlsson, A. H. E. Muller, *Macromolecules* **2004**, *37*, 7861.
[14] S. Y. Liu, N. C. Billingham, S. P. Armes, *Angew. Chem. Int. Ed.* **2001**, *40*, 2328.
[15] G. Gotzamanis, C. Tsitsilianis, *Macromol. Rapid Commun.* **2006**, *27*, 1757.
[16] S. Y. Liu, S. P. Armes, *Angew. Chem. Int. Ed.* **2002**, *41*, 1413.
[17] F. Bossard, T. Aubry, G. Gotzamanis, C. Tsitsilianis, *Soft Matter* **2006**, *2*, 510.
[18] E. A. G. Aniansson, S. N. Wall, *J. Phys. Chem.* **1974**, *78*, 1024.
[19] E. A. G. Aniansson, S. N. Wall, *J. Phys. Chem.* **1975**, *79*, 857.
[20] E. A. G. Aniansson, S. N. Wall, M. Almgren, H. Hoffmann, I. Kielmann, W. Ulbricht, R. Zana, J. Lang, C. Tondre, *J. Phys. Chem.* **1976**, *80*, 905.
[21] M. Kahlweit, *J. Colloid Interface Sci.* **1982**, *90*, 92.
[22] E. Lessner, M. Teubner, M. Kahlweit, *J. Phys. Chem.* **1981**, *85*, 1529.
[23] A. Halperin, S. Alexander, *Macromolecules* **1989**, *22*, 2403.
[24] Y. M. Wang, W. L. Mattice, D. H. Napper, *Langmuir* **1993**, *9*, 66.
[25] E. E. Dormidontova, *Macromolecules* **1999**, *32*, 7630.
[26] I. A. Nyrkova, A. N. Semenov, *Macromol. Theory Simul.* **2005**, *14*, 569.
[27] I. A. Nyrkova, A. N. Semenov, *Faraday Discuss.* **2005**, *128*, 113.
[28] Z. Y. Zhu, S. P. Armes, S. Y. Liu, *Macromolecules* **2005**, *38*, 9803.
[29] D. Wang, J. Yin, Z. Y. Zhu, Z. S. Ge, H. W. Liu, S. P. Armes, S. Y. Liu, *Macromolecules* **2006**, *39*, 7378.
[30] C. Honda, Y. Hasegawa, R. Hirunuma, T. Nose, *Macromolecules* **1994**, *27*, 7660.
[31] C. Honda, Y. Abe, T. Nose, *Macromolecules* **1996**, *29*, 6778.
[32] A. Patist, J. R. Kanicky, P. K. Shukla, D. O. Shah, *J. Colloid Interface Sci.* **2002**, *245*, 1.
[33] S. Perrier, P. Takolpuckdee, *J. Polym. Sci., Part A: Polym. Chem.* **2005**, *43*, 5347.
[34] Z. S. Ge, S. Z. Luo, S. Y. Liu, *J. Polym. Sci., Part A: Polym. Chem.* **2006**, *44*, 1357.
[35] S. H. Thang, Y. K. Chong, R. T. A. Mayadunne, G. Moad, E. Rizzardo, *Tetrahedron Lett.* **1999**, *40*, 2435.
[36] C. Wu, K. Q. Xia, *Rev. Sci. Instrum.* **1994**, *65*, 587.
[37] T. Haliloglu, I. Bahar, B. Erman, W. L. Mattice, *Macromolecules* **1996**, *29*, 4764.
[38] C. K. Smith, G. J. Liu, *Macromolecules* **1996**, *29*, 2060.
[39] Y. M. Wang, C. M. Kausch, M. S. Chun, R. P. Quirk, W. L. Mattice, *Macromolecules* **1995**, *28*, 904.
[40] R. Lund, L. Willner, D. Richter, E. E. Dormidontova, *Macromolecules* **2006**, *39*, 4566.
[41] R. Lund, L. Willner, J. Stellbrink, P. Lindner, D. Richter, *Phys. Rev. Lett.* **2006**, *96*, 068302.
[42] Z. S. Ge, Y. L. Cai, J. Yin, Z. Y. Zhu, J. Y. Rao, S. Y. Liu, *Langmuir* **2007**, *23*, 1114.
[43] C. Wu, X. P. Qiu, *Phys. Rev. Lett.* **1998**, *80*, 620.